Available online at www.sciencedirect.com
ScienceDirect
Trans. Nonferrous Met. Soc. China 31(2021) 1572−1586
Transactions of Nonferrous Metals Society of China
www.tnmsc.cn

Effect of Ca content and rheo-squeeze casting parameters on microstructure and mechanical properties of AZ91−1Ce−*x*Ca alloys

Ran XIAO, Wen-cai LIU, Guo-hua WU, Liang ZHANG, Bao-liang LIU, Wen-jiang DING

National Engineering Research Center of Light Alloy Net Forming and
Key State Laboratory of Metal Matrix Composite, School of Materials Science and Engineering,
Shanghai Jiao Tong University, Shanghai 200240, China

Received 2 June 2020; accepted 28 March 2021

Abstract: The microstructure, mechanical properties and flame resistance behavior of the AZ91−1Ce alloys with different Ca additions were firstly investigated. Then, the effect of processing parameters, including applied pressures and rotation speeds, on the microstructure and mechanical properties of the rheo-squeeze casting AZ91−1Ce−2Ca alloy was studied. The results indicate that with the increase of Ca content, the microstructure is refined and the flame resistance of the AZ91−1Ce−*x*Ca alloys increases. But when the Ca content exceeds 1 wt.%, with the Ca content increasing, the mechanical properties of the AZ91−1Ce−*x*Ca alloys reduce rapidly. For rheo-squeeze casting process, the increase of applied pressure and rotation speed can both bring about significant refinement in the microstructure of the AZ91−1Ce−2Ca alloy and reduction of the porosity, so the mechanical properties increase. Compared to conventional casting, the AZ91−1Ce alloy with the addition of 2 wt.% Ca by rheo-squeeze casting not only guarantees the oxidation resistance (801 °C), but also improves mechanical properties.
Key words: Ca; AZ91−1Ce alloy; oxidation resistance; rheo-squeeze casting

1 Introduction

As the lightest metal engineering material, magnesium alloy has the advantages of high specific strength, high flexibility, and good magnetic shielding properties, and is widely used in automotive, aerospace and medical industry [1,2]. Among the magnesium alloys, Mg−Al series alloy such as AZ91 alloy is the most successfully developed and widely used magnesium alloy, due to the combination of good mechanical properties and comprehensive casting [3,4].

However, AZ91 alloy is easy to burn and oxidize during melting and casting process, resulting in limiting its wider applications in industry [5,6]. It is demonstrated that micro-alloying with calcium (Ca) is a feasibility way to improve the flame resistance of AZ91 alloy [7]. Ca is an appropriate flame-retardant element. It is also found that the flame-retardant effect of Ce and Ca combined is better than that of single addition. Considering the high price of Ce element, 1% Ce is added to AZ91 alloy in this work [8,9]. However, the high addition of Ca content decreases the ultimate tensile strength (UTS) and elongation (E_f) of AZ91−1Ce alloy at ambient temperature [10]. Therefore, it is essential to develop effective approaches to improve the mechanical properties of AZ91−Ca−Ce alloy when ensuring excellent flame retardant properties.

Semi-solid metal (SSM) process which combines the advantages of forging method and traditional casting can get fine and uniform non-dendrite microstructures by gas bubbling stirring [11,12]. Rheoforming involves the direct

Corresponding author: Wen-cai LIU, Tel: +86-21-54742630, Fax: +86-21-34202794, E-mail: liuwc@sjtu.edu.cn
DOI: 10.1016/S1003-6326(21)65599-1

component shaping of semi-solid slurry by squeeze casting or die casting. Because squeeze casting (SQC) is a combination of forging and casting, the mold filling and solidification of semi-solid slurry are achieved under applied pressure during rheo-squeeze casting process. Therefore, rheo-squeeze casting process can manufacture near-net-shape castings with low porosity and good mechanical properties [13,14].

Many researchers have carried out research work on rheo-squeeze casting of AZ91 alloy and proved that the rheo-squeeze casting is an effective way to produce high-performance AZ91 alloy. For example, ZHANG et al [15] studied the preparation and rheo-squeeze casting of semi-solid AZ91−2Ca alloy by gas bubbling process. But until now, there has not been much research work on effect of Ca content and rheo-squeeze casting parameters (especially the rotation speed) on microstructure and mechanical properties of AZ91−Ce−Ca alloy.

Accordingly, in this study, the effect of Ca content on flame retardance, microstructure and mechanical properties of the gravity casting AZ91−1Ce−*x*Ca alloys was investigated to determine the calcium content, ensuring the flame resistance and mechanical properties of the AZ91−1Ce−*x*Ca alloys. Then, the effects of applied pressure and rotation speed on microstructure and mechanical properties of the rheo-squeeze casting AZ91−1Ce−2Ca alloy were investigated. The mechanisms of refinement in microstructure and improvement in oxidation resistance and mechanical properties were discussed correlated with microstructure characterization.

2 Experimental

2.1 Materials and sample preparation

Commercial AZ91D ingots, pure metal Ca (99.9%) and Mg−90Ce (wt.%) master alloy were used to produce AZ91−1Ce−*x*Ca (wt.%) alloys. The samples in this work were used to prepare gravity casting AZ91−1Ce−*x*Ca (*x*=0, 1, 2, 3, wt.%) and rheo-squeeze casting AZ91−1Ce−2Ca (wt.%) alloys. The actual chemical compositions of both gravity casting and rheo-squeeze casting alloys were determined using inductively coupled plasma-atomic emission spectrometry (ICP-AES) and the results are presented in Table 1. First of all, the AZ91 ingot was melted by a stainless steel crucible heating in an electric resistance furnace, protected with a mixed gas atmosphere of 1% SF_6 and 99% CO_2 (volume fraction). AZ91D ingot was heated to 720 °C and when it melted completely, Mg−90Ce master alloy was added into the melt and stirred for 5 min to achieve homogeneous chemical distribution. After that, Ca was added at 680 °C and stirred for 5 min. Before gravity casting and rheo-squeeze casting, the melt was isothermally held at 720 °C for 30 min to ensure that all the alloying elements were completely dissolved.

Table 1 Chemical compositions of AZ91−1Ce−*x*Ca alloys used in this study (wt.%)

Alloy	Ce	Ca	Al	Zn	Mg
AZ91−1Ce (Gravity casting)	1.08	−	8.00	0.53	Bal.
AZ91−1Ce−1Ca (Gravity casting)	1.13	0.87	8.53	0.62	Bal.
AZ91−1Ce−2Ca (Gravity casting)	1.21	1.95	8.67	0.59	Bal.
AZ91−1Ce−3Ca (Gravity casting)	1.06	3.17	8.34	0.55	Bal.
AZ91−1Ce−2Ca (Rheo-squeeze casting)	1.02	2.10	7.61	0.50	Bal.

The equipment used for blowing Ar gas and rheo-squeeze casting process is visually shown in Fig. 1. The diameter of mould chamber or rheocasting sample in Fig. 1(b) is 60 mm. The rheo-squeeze casting parameters varied in this study are shown in Table 2. The liquidus and solidus temperatures of the AZ91−1Ce−2Ca alloy are 480 and 599 °C, respectively. Before rheo-squeeze casting, the mold was preheated to 250 °C. In the first round, applied pressure was varied from 0 to 130 MPa, while rotation speed, gas flow rate and stirring end temperature were kept at 120 r/min, 6 L/min and 587 °C, respectively. In the second round, applied pressure, gas flow rate and stirring end temperature were kept at 130 MPa, 6 L/min and 587 °C, respectively, while the rotation speed was varied from 0 to 120 r/min.

2.2 Ignition point and oxidation resistance tests

For the samples of the gravity casting AZ91−1Ce−*x*Ca (*x*=0, 1, 2, 3, wt.%) alloys, ignition tests were carried out on cubic specimens with size of 15 mm × 15 mm × 15 mm, polished with 1000, 1500 and 3000 grit SiC papers. Ignition tests were

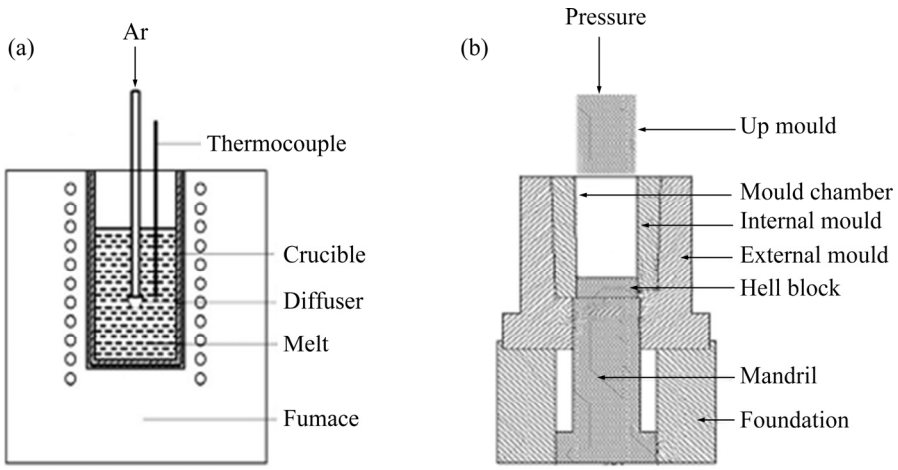

Fig. 1 Illustration of gas-bubbling process (a) and rheo-squeeze casting process (b)

Table 2 Processing parameters used in rheo-squeeze casting process

Applied pressure/ MPa	Rotation speed/ ($r \cdot min^{-1}$)	Gas flow rate/ ($r \cdot min^{-1}$)	Stirring end temperature/ °C
0 70 100 130	130	6	587
120	120 0 60 120	6	587

performed by inserting a K-type thermocouple into a hole drilled at the center of the sample (Fig. 2), and heating the sample at a rate of 5 °C/min using an electrical furnace. The combustion heat was large enough to cause a steep rise on the temperature−time curve of the samples so that the knee point was defined as ignition temperature of alloy [17]. The oxidation experiments of AZ91−1Ce alloy and AZ91−1Ce−2Ca alloy were carried out, respectively, in air under isothermal conditions at three different temperatures (425, 450 and 475 °C) for 30 min.

2.3 Microstructure analysis

First of all, microstructure specimens were cut from gravity casting samples and rheo-squeeze casting samples by an electric-sparking wire-cutting machine and prepared with standard metallographic procedures. Then, the microstructure characterization of the tested alloy was carried out by an optical microscope (OM, ZEISS) and a scanning electron microscope (SEM, Phenom XL)

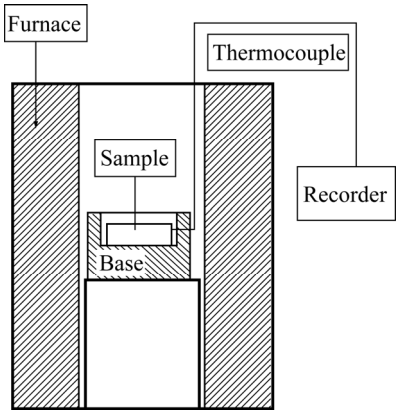

Fig. 2 Schematic diagram of experimental device for measurement of ignition temperature [16]

equipped with an energy-dispersive spectroscope (EDS) to determine the local chemical compositions. The quantitative image analysis software (image-pro plus v6.0) was used to make quantitative metallographic analysis. The phase compositions were analyzed using X-ray diffraction technique (XRD; Ultima IV).

2.4 Tensile testing

A Zwick/Roell Z020 tensile machine was used for ambient temperature tensile testing and the cross-head speed was 1 mm/min. The gage dimensions of the tensile samples were 54.5 mm × 15 mm × 2 mm.

3 Results

3.1 Effect of Ca content on gravity casting AZ91−1Ce−*x*Ca alloys

Figure 3 shows the XRD patterns of the

gravity casting AZ91−1Ce alloys with different Ca contents. According to the XRD results, the AZ91−1Ce alloy is mainly composed of α-Mg, Al_4Ce and β-$Mg_{17}Al_{12}$ phases. With the addition of Ca content, the AZ91−1Ce−xCa (x=1, 2, 3, wt.%) alloys consist of α-Mg, Al_4Ce, β-$Mg_{17}Al_{12}$ and Al_2Ca phases.

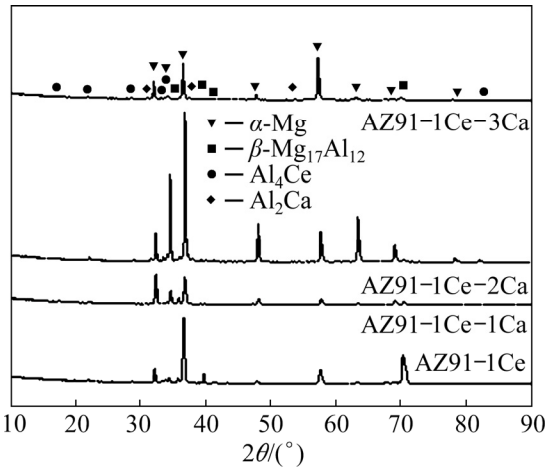

Fig. 3 XRD patterns of gravity casting AZ91−1Ce alloys with different Ca contents

Figure 4 shows the microstructure of the gravity casting AZ91−1Ce alloys with different Ca contents. Al_2Ca phase is black-lamellar, $Mg_{17}Al_{12}$ phase is light-colored skeleton shaped, and Al_4Ce is white-dotted. When the Ca content increases from 0 to 1%, the refinement in the microstructures is clearly visible. But with the Ca content increasing from 1% to 3%, the grain structure coarsens, and the amount of the $Mg_{17}Al_{12}$ phase decreases while that of Al_2Ca phase increases.

In order to further clarify the distribution of Ca element in the gravity casting AZ91−1Ce−xCa alloys, the image mapping analysis is conducted by EDS. Figure 5 presents the image mapping results of the gravity casting AZ91−1Ce alloys with different Ca contents. Secondary electron and backscatter images were used respectively at the same site. Al_2Ca phase has large network structure, $Mg_{17}Al_{12}$ phase is gray skeleton shaped, and Al_4Ce is bright white acicular. With the Ca content increasing, the formation of $Mg_{17}Al_{12}$ phase is suppressed, and the formation of Al_2Ca phase is promoted significantly and Ca element is distributed at Al_2Ca phase which has large network structure and the size of which is not uniform. It is also observed that the amount of Ca element dissolved in the α-Mg matrix is very low in all samples. In addition, when Ca content increases from 0 to 3 wt.%, the morphology of eutectic changes from separated to connect reticular along the grain boundaries.

The effect of Ca content on mechanical properties of the gravity casting AZ91−1Ce−xCa alloys is presented in Fig. 6 and Table 3. With the increase of Ca content, the mechanical properties of the AZ91−1Ce−xCa alloys first increase and then decrease. When Ca content is 1%, the yield strength (YS), ultimate tensile strength (UTS) and elongation (E_f) of the alloy reach the maximum values of 124.2 MPa, 195.4 MPa, and 3.2%, respectively. Compared with the AZ91−1Ce alloy, the AZ91−1Ce−3Ca alloy exhibits an increase of 6.7% in YS and a decrease of 21.5% and 55.2% in UTS and E_f, respectively.

3.2 Effect of Ca on oxidation resistance of gravity casting AZ91−1Ce alloys

Typical temperature vs time curves of ignition point testing are shown in Fig. 7. It is observed that the tested average ignition point of the AZ91−1Ce alloy is 597 °C. With the Ca content increasing, the ignition point of the AZ91−Ce−Ca alloy increases. It is noticeable that the AZ91−1Ce alloy containing 3 wt.% Ca is 900 °C. The increase in ignition temperature implies that the oxidation behavior of the AZ91 alloy in solid-state is changed by the Ca addition, and the ignition and burning of the AZ91 alloy are suppressed as well. Considering that the melting temperature of the AZ91 alloy doesn't exceed 750 °C, the optimized result is that the AZ91−1Ce alloy is added by 2 wt.% Ca.

Figure 8 shows the surface morphologies of the AZ91−1Ce and AZ91−1Ce−2Ca alloys after being oxidized for 30 min at 425, 450 and 475 °C. In Fig. 8(a), a thin oxide film with black oxide product in some region is formed on the AZ91−1Ce sample at 425 °C, while AZ91−1Ce−2Ca sample displays a regular surface. From Figs. 8(b, c), when the temperature increases, the oxidation becomes severer and the surfaces of the samples are covered by a large number of nodular reaction products. It is obvious that wrinkles on the AZ91−1Ce alloy increase and cracks formed on the AZ91−1Ce alloy grow significantly. Furthermore, compared with Figs. 8(a−c), the oxidation is suppressed after Ca is added, as shown in Figs. 8(d−f).

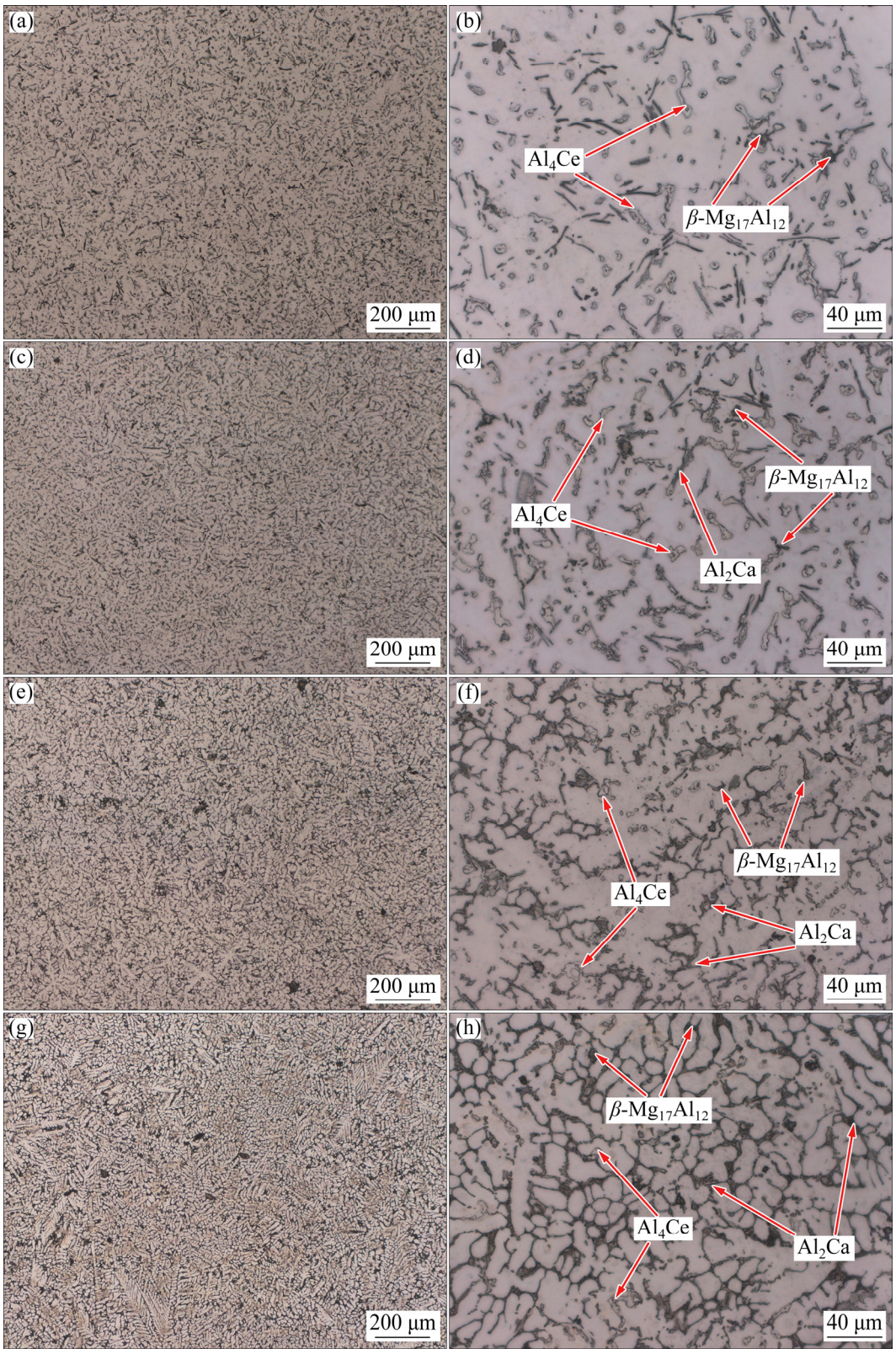

Fig. 4 Low and high magnification OM images of gravity casting AZ91−1Ce alloys with different Ca contents: (a, b) AZ91−1Ce; (c, d) AZ91−1Ce−1Ca; (e, f) AZ91−1Ce−2Ca; (g, h) AZ91−1Ce−3Ca

3.3 Effect of applied pressure on rheo-squeeze casting AZ91−1Ce−2Ca alloy

Figure 9 shows the microstructural evolution of the rheo-squeeze casting alloy with the increase of pressure from 0 to 130 MPa. The microstructures are composed of internally solidified grains (ISGs,

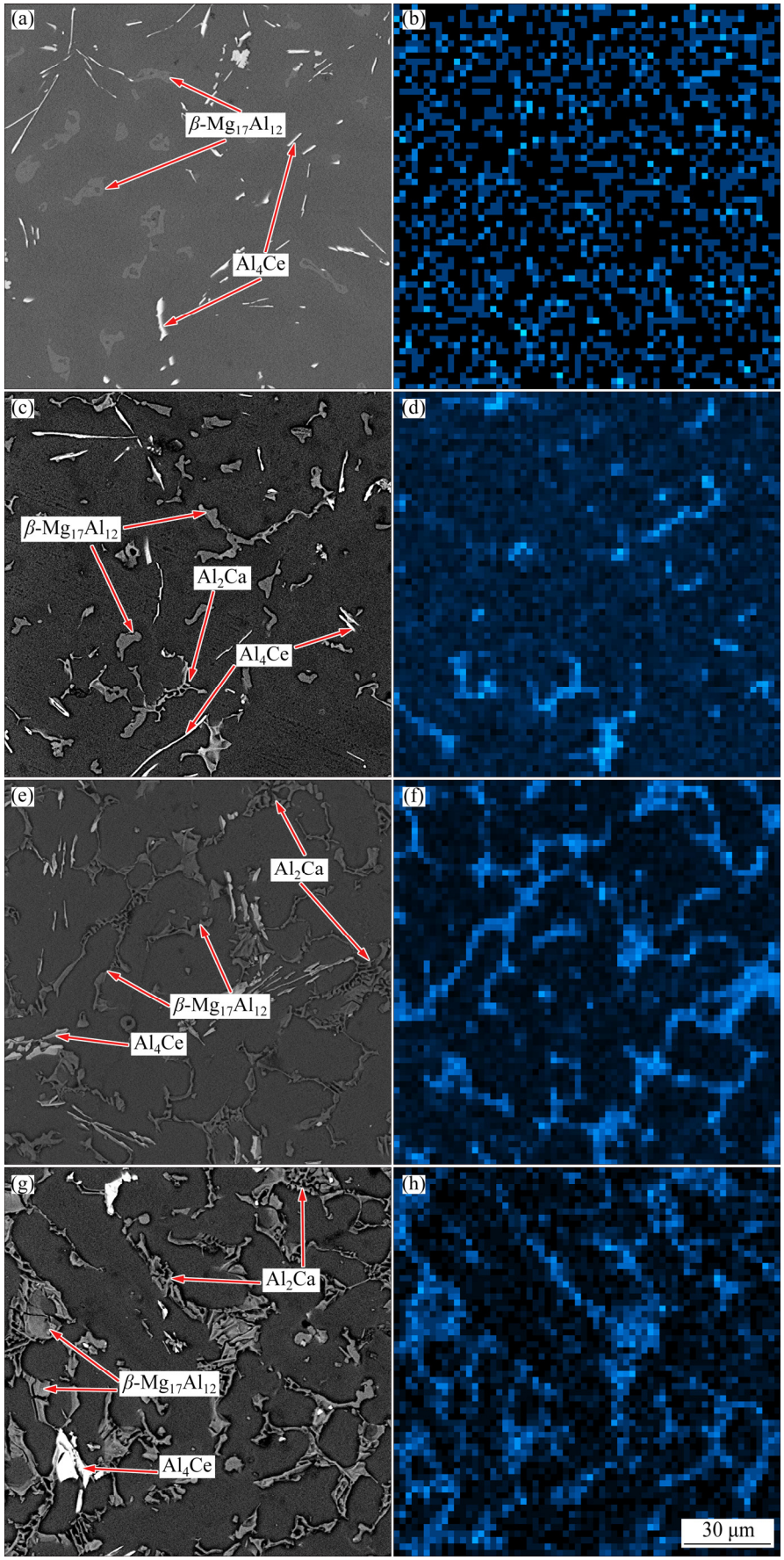

Fig. 5 Image mapping results (secondary electron and backscattered electron) of gravity casting AZ91−1Ce−*x*Ca alloys: (a, b) AZ91−1Ce; (c, d) AZ91−1Ce−1Ca; (e, f) AZ91−1Ce−2Ca; (g, h) AZ91−1Ce−3Ca

Table 3 Mechanical properties of gravity casting AZ91−1Ce−*x*Ca alloys

Ca content/wt.%	YS/MPa	UTS/MPa	E_f/%
0	106.1	181.1	2.9
1	124.2	195.4	3.2
2	115.5	156.6	1.4
3	113.2	142.1	1.3

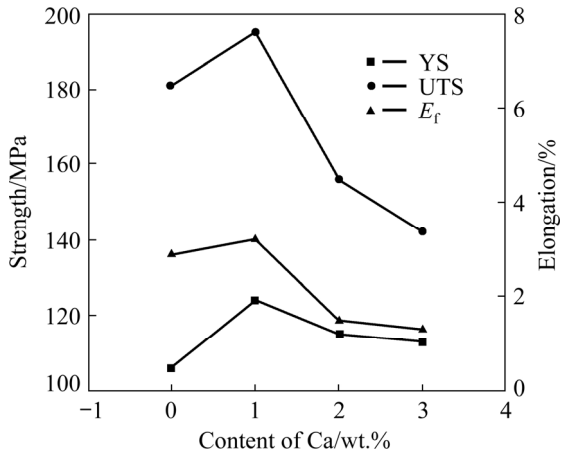

Fig. 6 Effect of Ca content on YS, UTS and E_f of gravity casting AZ91−1Ce alloys

the finer grains) and externally solidified grains (ESGs, the larger grains). The ESGs form primarily during slurry preparation, while the ISGs correspond to fine and round grains that nucleate and grow in the mould cavity.

As seen in Figs. 9(a, b), when semi-solid slurry of the AZ91−1Ce−2Ca alloy solidifies without applied pressure, the ISGs and the ESGs are both coarse dendrites and it is difficult to distinguish α-Mg particles from secondary α-Mg phase. However, when the applied pressure reaches 70 MPa and above, as seen in Figs. 9(c−h), the size of primary ESGs and ISGs decreases and their morphology tends to keep round. This indicates that the secondary growth of primary α-Mg particles during rheo-squeeze casting is restricted under high level of applied pressure. As for the residual melt, increase of applied pressure brings significant refinement in microstructure.

Figure 10 shows the SEM images of the rheo-squeeze casting AZ91−1Ce−2Ca alloy under different pressures. When the pressure increases

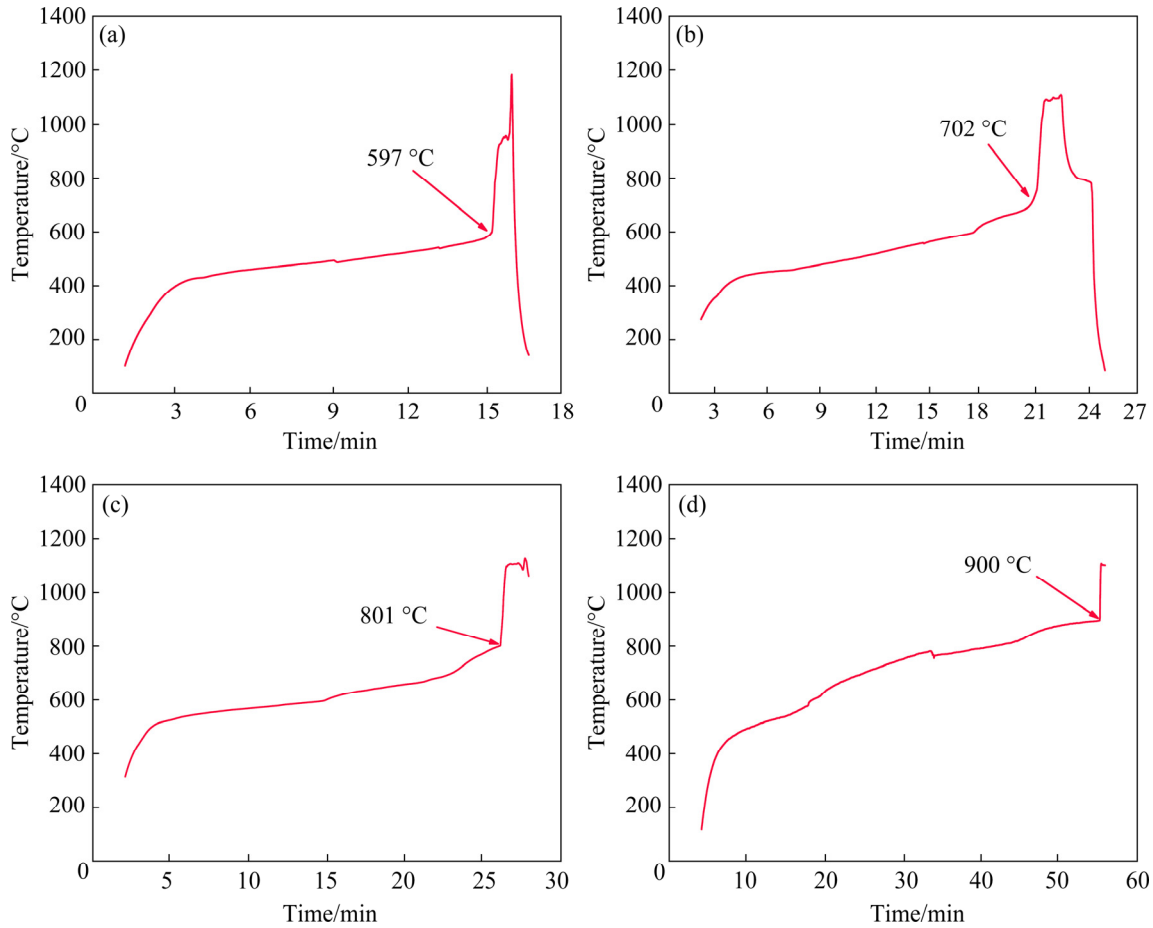

Fig. 7 Typical temperature vs time curves of ignition point test with different Ca contents in AZ91−1Ce alloys: (a) AZ91−1Ce; (b) AZ91−1Ce−1Ca; (c) AZ91−1Ce−2Ca; (d) AZ91−1Ce−3Ca

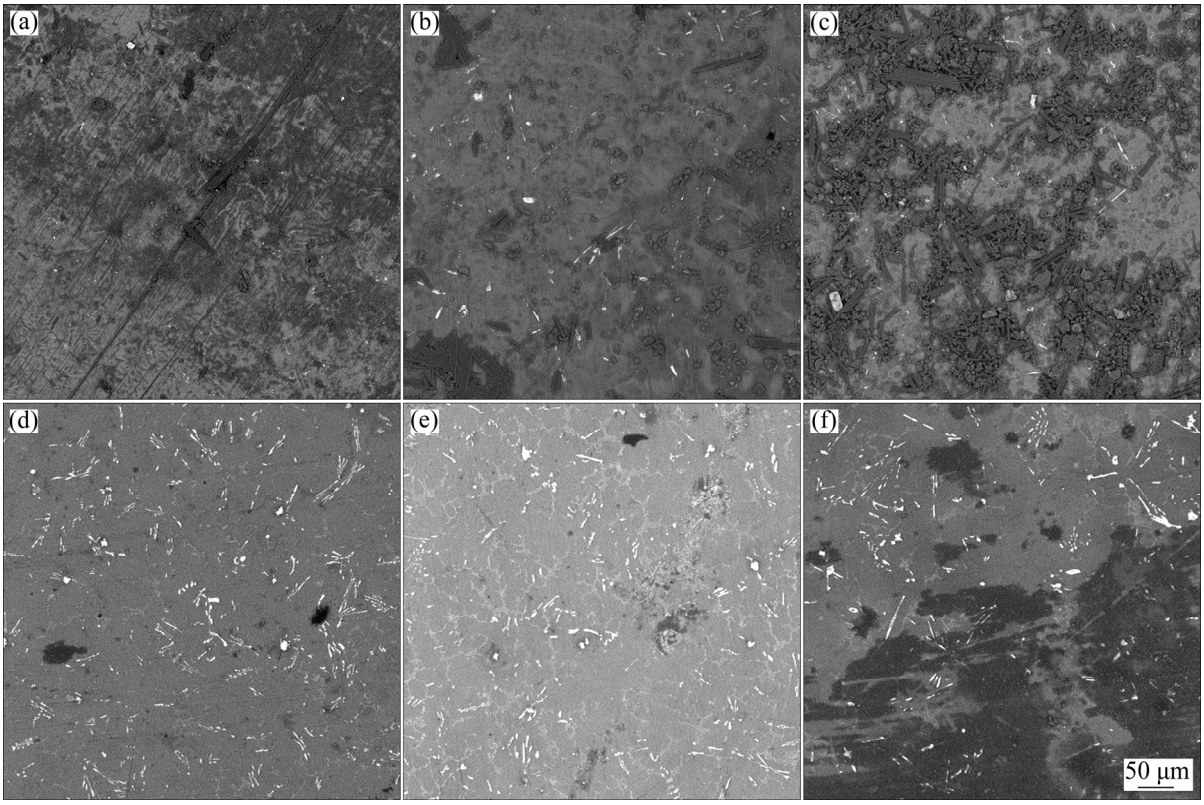

Fig. 8 SEM images showing oxide scales formed after oxidation for 30 min: (a) AZ91−1Ce, 425 °C; (b) AZ91−1Ce, 450 °C; (c) AZ91−1Ce, 475 °C; (d) AZ91−1Ce−2Ca, 425 °C; (e) AZ91−1Ce−2Ca, 450 °C; (f) AZ91−1Ce−2Ca, 475 °C

from 0 to 130 MPa, the second phase of the rheo-squeeze casting AZ91−1Ce−2Ca alloy is obviously refined, and especially the layer thickness of Al_2Ca phase is reduced significantly. Under the pressure of 130 MPa, the compounds along grain boundaries are obviously refined and distributed uniformly. With the increase of applied pressure, dendritic arm spacing decreases and finer dendrites are observed.

The tensile properties of rheo-squeeze casting AZ91−1Ce−2Ca samples under different pressures are shown in Fig. 11 and Table 4. An increase in pressure brings significant improvements in the YS and UTS, and a slight improvement in the elongation. The YS, UTS and E_f of the rheo-squeeze casting samples under the pressure of 130 MPa are 130.1 MPa, 189.1 MPa and 2.4%, respectively. Additionally, the slurry prepared for rheo-squeeze casting was used to produce the gravity casting AZ91−1Ce−2Ca alloy. The YS, UTS and E_f of the gravity casting AZ91−1Ce−2Ca alloy are 115.1 MPa, 145.1 MPa and 1.1%, respectively, lower than those of the rheo-squeeze casting AZ91−1Ce−2Ca alloy.

3.4 Effect of rotation speed on rheo-squeeze casting AZ91−1Ce−2Ca alloy

Figure 12 shows the microstructural evolution of the rheo-squeeze casting AZ91−1Ce−2Ca alloy with the increase of rotation speed from 0 to 120 r/min. When the rotation speed reaches 60 r/min, the morphology of primary α-Mg phase is dominated by a fine and globular-like structure. As the rotation speed increases, the average particle size has a tendency of decrease and the morphology tends to keep round. Compared with no rotation, the finer microstructures can be obtained under the rotating gas bubble stirring treatment.

Figure 13 shows the SEM images of the rheo-squeeze casting AZ91−1Ce−2Ca alloy under different rotation speeds. When the rotation speed increases from 0 to 120 r/min, the second phase of the rheo-squeeze casting AZ91−1Ce−2Ca alloy is continuously refined, and the layer thickness of Al_2Ca phase is reduced. It is also observed that the rotation speed leads to a uniform distribution of

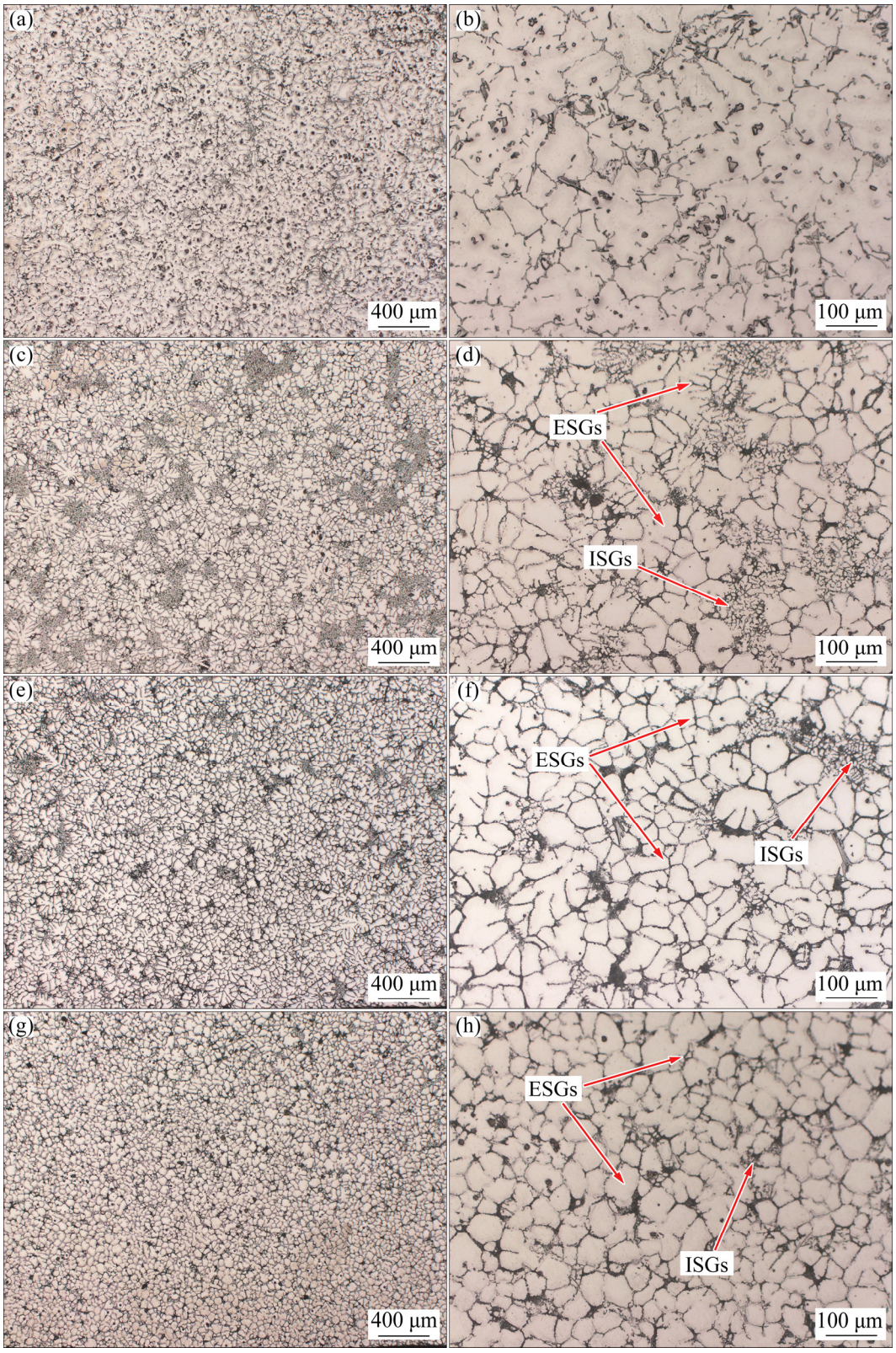

Fig. 9 Low and high magnification OM images of rheo-squeeze casting AZ91−1Ce−2Ca alloy prapared by gas bubbling process under different applied pressures: (a, b) 0 MPa; (c, d) 70 MPa; (e, f) 100 MPa; (g, h) 130 MPa

intermetallic compounds.

The tensile properties of the rheo-squeeze casting AZ91−1Ce−2Ca samples under different rotation speeds are shown in Fig. 14 and Table 5. It is found that the increase of rotation speed brings about significant improvement in mechanical

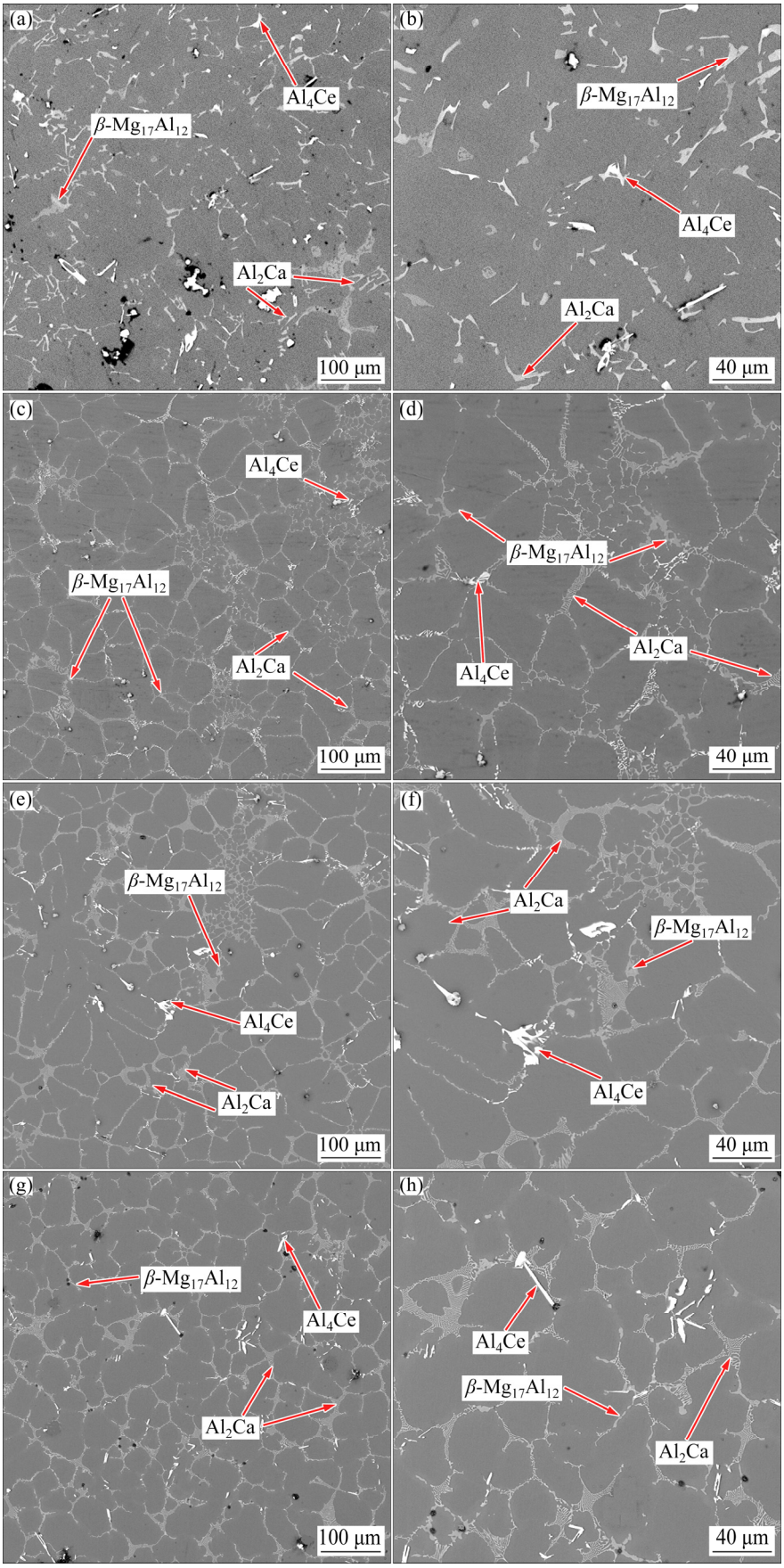

Fig. 10 Low and high magnification SEM images of rheo-squeeze casting AZ91−1Ce−2Ca alloy prepared under different pressures: (a, b) 0 MPa; (c, d) 70 MPa; (e, f) 100 MPa; (g, h) 130 MPa

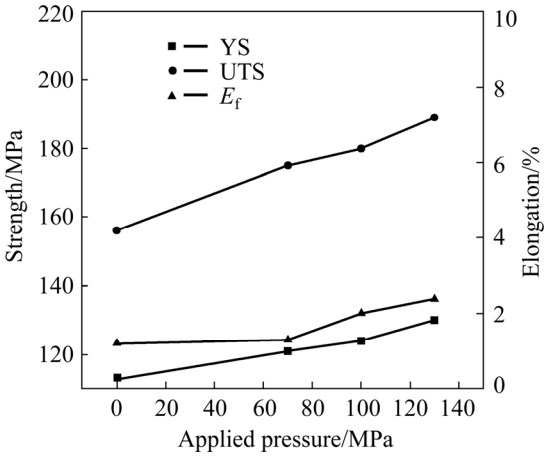

Fig. 11 Effect of applied pressure on YS, UTS and E_f of rheo-squeeze casting AZ91−1Ce−2Ca alloy

Table 4 Mechanical properties of rheo-squeeze casting AZ91−1Ce−2Ca alloy prepared under different pressures

Pressure/MPa	YS/MPa	UTS/MPa	E_f/%
0	115.1	145.1	1.1
70	121.3	175.1	1.3
100	124.2	180.2	2.0
130	130.1	189.1	2.4

properties. The YS, UTS and E_f of the rheo-squeeze casting samples under the rotation speed of 120 r/min are 130.1 MPa, 189.1 MPa and 2.4%, which are improved by 13%, 26% and 118%, respectively, compared with those of the samples without applied pressure.

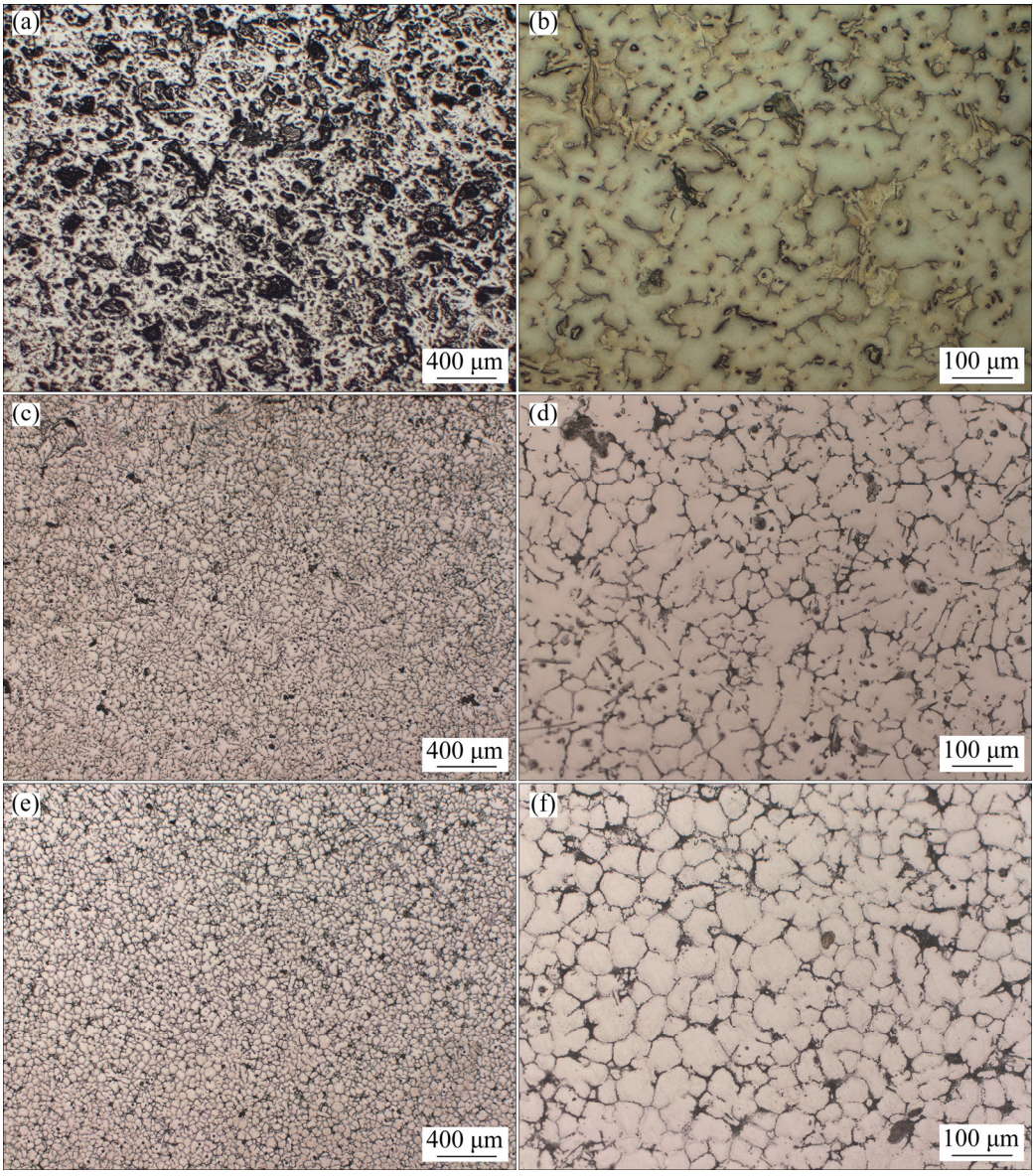

Fig. 12 Low and high magnification OM images of rheo-squeeze casting AZ91−1Ce−2Ca alloy prepared by gas bubbling process under different rotation speeds: (a, b) 0 r/min; (c, d) 60 r/min; (e, f) 120 r/min

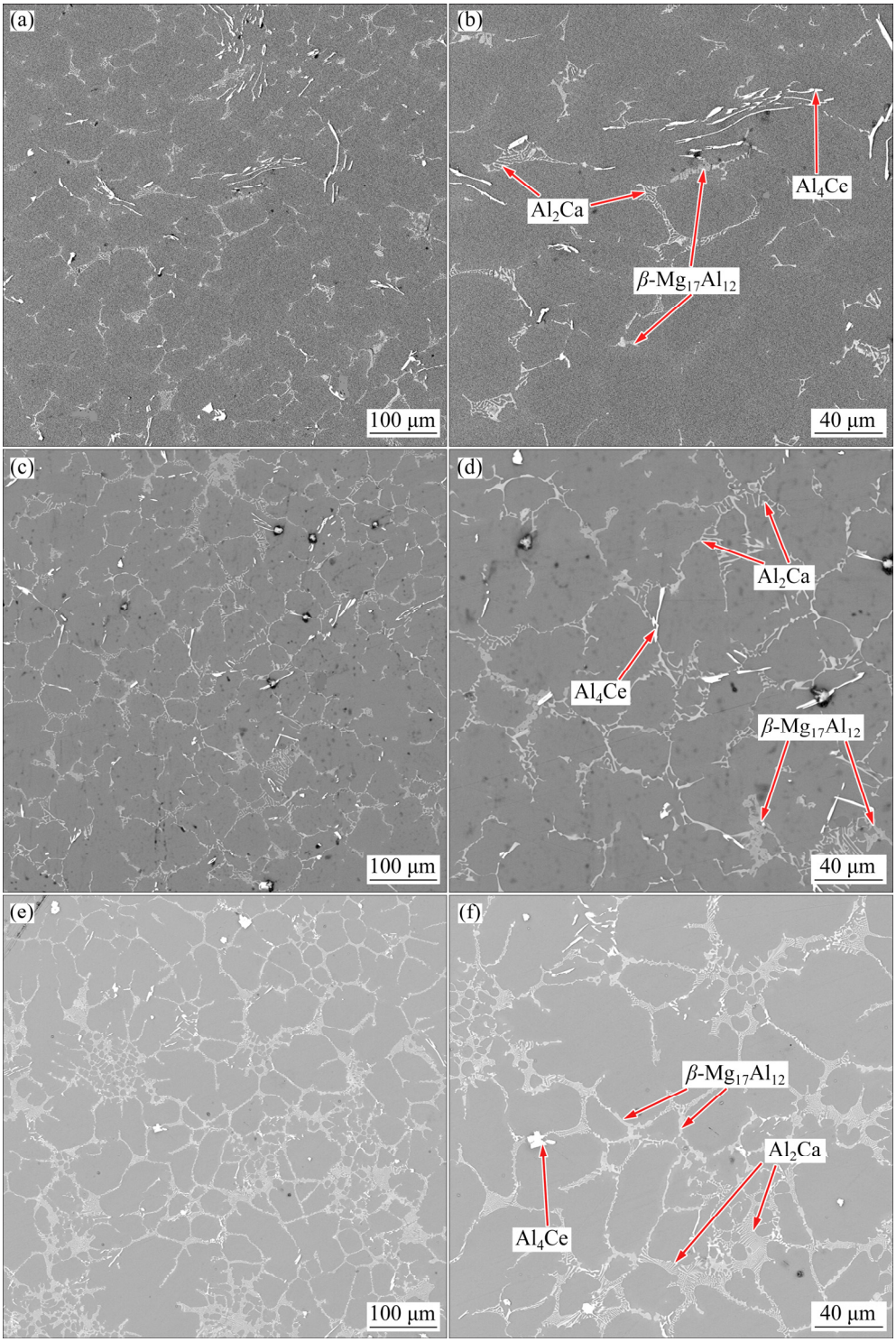

Fig. 13 Low and high magnification SEM images of rheo-squeeze casting AZ91−1Ce−2Ca alloy prepared under different rotation speeds: (a, b) 0 r/min; (c, d) 60 r/min; (e, f) 120 r/min

4 Dissusion

4.1 Effect of Ca content on microstructure and properties of gravity casting AZ91−1Ce−*x*Ca alloys

When Ca content is less than 1%, the addition of Ca to the AZ91−1Ce alloy can significantly refine the gravity casting microstructures of alloy. Generally, with the Ca content increasing, the formation of second phase such as Al_2Ca can act as potential nucleation sites for Mg and give rise to the constitution undercooling, which is recognized as the growth restriction factor(GRF) [18,19].

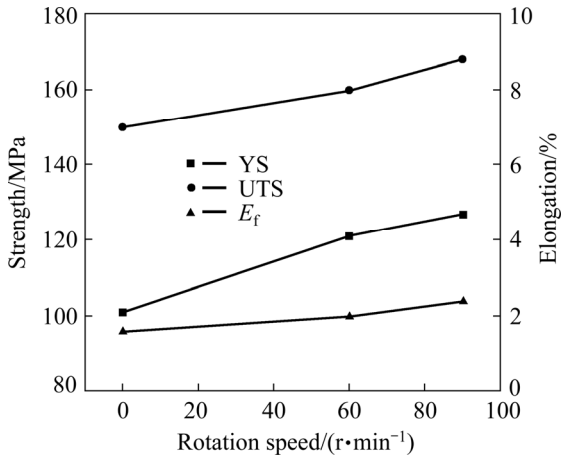

Fig. 14 Effect of rotation speed on YS, UTS and E_f of rheo-squeeze casting AZ91−1Ce−2Ca alloy

Table 5 Mechanical properties of rheo-squeeze casting AZ91−1Ce−2Ca alloy under different rotation speeds

Rotation speed/(r·min^{-1})	YS/MPa	UTS/MPa	E_f/%
0	115.6	150.4	1.1
60	122.3	164.4	1.3
120	130.1	189.1	2.4

According to HUNT [20], GRF can be defined as follows:

$$\mathrm{GRF}=\sum m_i c_{0,i}(k_i-1) \tag{1}$$

where m_i is the slope of the liquidus line, c_0 is the initial compositions, and k_i is the equilibrium partition coefficient for element i. A large GRF can result in a large growth restriction in the grain. Due to the strong segregating power of Ca, GRF increases, and consequently it can refine the microstructure of magnesium alloy significantly [21].

With Ca content increasing from 0 to 1%, the yield strength of the AZ91−1Ce−xCa alloys at ambient temperature increases, which can be explained by the Hall−Petch correlation [22]. When the Ca content increases from 1.0% to 3.0%, the addition of Ca results in the formation of Al_2Ca phase and inhibits the precipitation of $Mg_{17}Al_{12}$ phase. For the AZ91−1Ce alloy, the $Mg_{17}Al_{12}$ phase is considered as the main strengthening phase.With increasing Ca content, the more the amount of connected network Al_2Ca phase is, the less the amount of $Mg_{17}Al_{12}$ phase is. Because Al_2Ca phase is more brittle than $Mg_{17}Al_{12}$ phase and easy to break, worsening the ductility of the AZ91−1Ce−xCa alloys, the addition of Ca results in a continuous decreas in mechanical properties at ambient temperature.

With the addition of Ca, the formation of Al_2Ca phase with high ignition point suppresses the formation of the low ignition point eutectic phase, $Mg_{17}Al_{12}$, resulting in increasing the ignition point of the AZ91−1Ce−xCa alloys. According to CHOI et al [23] and CHEN et al [24], CaO and MgO, having the role of effective barrier preventing further oxidation, are formed on the surface of the molten AZ91−1Ce−xCa alloys, consequently increasing the oxidation resistance of the AZ91−1Ce−xCa alloys.

4.2 Effect of applied pressure and rotation speed on mechanical properties of rheo-squeeze casting AZ91−1Ce−2Ca alloy

In this study, it is evidently observed that the increase of applied pressure brings about significant refinement in the microstructure of the rheo-squeeze casting AZ91−1Ce−2Ca samples. Till now, there are two theories trying to explain the mechanism of grain refinement under applied pressure. Firstly, high pressure could make the mould and the components contact more closely, increasing the heat transfer coefficient between the die surface and the slurry [25,26]. With the increase of applied pressure, the improvement of heat transfer and cooling heat becomes more noticeable, resulting in the refinement in microstructure. Alternatively, the application of pressure could raise the liquidus temperature of the alloy and lead to higher degree of undercooling, deduced by considering the Clausius−Clapeyon equation [25]:

$$\frac{\Delta T_f}{\Delta P}=\frac{T_f(V_l-V_s)}{\Delta H_f} \tag{2}$$

where T_f is the equilibrium freezing temperature, V_l and V_s are the specific volumes of the liquid and solid, respectively, P is the applied pressure, and ΔH_f is the latent heat of fusion.

The effect of pressure on the freezing point may be roughly estimated as follows:

$$P=P_0\exp\left(\frac{-\Delta H_f}{RT_f}\right) \tag{3}$$

where P_0, ΔH_f and R are constants. According to Eq. (2), T_f should increase with pressure increasing. The increase of T_f can make a higher undercooling compared with conventional castings and promote

the nucleation rate, which is favorable for grain refinment.

The yield stress σ_y is related to the grain size by Eq. (4):

$$\sigma_y=\sigma_0+Kd^{-1/2} \quad (4)$$

where σ_0 and K are constants. σ_0 is a friction stress, which includes contributions from solutes and particles but not from dislocations, i.e. σ_0 is the flow stress of an undeformed single crystal orientated for multiple slip or approximately the yield stress of a very coarse-grained, untextured polycrystal. From Eq. (4), the refinement of the grain is beneficial to its mechanical properties.

With the applied pressure increasing, the improvement in mechanical properities of the AZ91−1Ce−2Ca alloy achieved can be partially attributed to the grain refinement of α-Mg particles and residual melt. Another possible factor is that the formation of gas pores and shrinkage is inhibited when solidified under appied pressure, increasing the densification, which is beneficial to the final mechanical properties.

In this study, it is evidently observed that the increase of rotation speed brings about significant refinement in the microstructure of the rheo-squeeze casting AZ91−1Ce−2Ca samples. The vigorous stirring provides significant temperature disturbances around the dendrite root and causes dendrite fragmentation, resulting in the refinment of the microstructure and a uniform distribution of intermetallic compounds, which is beneficial to the mechanical properities of the AZ91−1Ce−2Ca alloy [26].

5 Conclusions

(1) When the Ca content increases from 0 to 3%, the mechanical properties of the AZ91−1Ce−*x*Ca alloys first increase and then decrease, and the ignition point increases gradually. When the Ca content is 1%, the yield strength, ultimate tensile strength and elongation of the alloy reach the maximum values, 124.2 MPa, 195.4 MPa and 3.2%, respectively. When the Ca content is 2%, its ignition point is 801 °C. Combined with these two aspects, considering that AZ91 alloy is normally smelted at 700−800 °C, the Ca content is optimized to be 2%.

(2) Increase of applied pressure and rotation speed refines microstructure and improves mechanical properties. Within the experimental parameters of this work, when the rotation speed and applied pressure are 120 r/min and 130 MPa, respectively, the yield strength, ultimate tensile strength and elongation of the AZ91−1Ce−2Ca alloy reach the maximum values, 130.1 MPa, 189.1 MPa and 2.4%, respectively.

Acknowledgments

The authors are grateful for the financial supports from National Natural Science Foundation of China (Nos. 51775334, 51771115, U2037601), and Research Program of Joint Research Center of Advanced Spaceflight Technologies, China (No. USCAST2020-14).

References

[1] SUN Yue-hua, WANG Ri-chu, PENG Chao-qun, FENG Yan, YANG Ming. Recent progress in Mg−Li matrix composites [J]. Transactions of Nonferrous Metals Society of China, 2019, 29(1): 1−14.

[2] JIA Qing-gong, ZHANG Wen-xin, SUN Yi, XU Chun-xiang, ZHANG Jin-shan, KUAN Jun. Microstructure and mechanical properties of as-cast and extruded biomedical Mg−Zn−Y−Zr−Ca alloy at different temperatures [J]. Transactions of Nonferrous Metals Society of China, 2019, 29(3): 515−525.

[3] ASL K M, TARI A, KHOMAMIZADEH F. The effect of different content of Al, RE and Si element on the microstructure, mechanical and creep properties of Mg−Al alloys [J]. Mater Sci Eng A, 2009, 523(1−2): 1−6.

[4] AZZEDDINE H, ABDESSAMEUD S, ALILI B, BOUMEERZOUG Z, BRADAI D. Effect of grain boundary misorientation on discontinuous precipitation in an AZ91 alloy [J]. Bulletin of Materials Science, 2011, 34: 1471−1476.

[5] LEE Dong-bok, HONG Lee-seok, KIM Young-jig. Effect of Ca and CaO on the high temperature oxidation of AZ91D Mg alloys [J]. Materials Transactions, 2008, 49(5): 1084−1088.

[6] AMBAT R, AUNG N N, ZHOU Wei. Evaluation of microstructural effects on corrosion behaviour of AZ91D magnesium alloy [J]. Corrosion Science, 2000, 42(8): 1433−1455.

[7] FAN Jian-feng, YANG Chang-lin, XU Bing-she. Effect of Ca and Y additions on oxidation behavior of magnesium alloys at high temperatures [J]. Journal of Rare Earths, 2012, 30(5): 105−110.

[8] RAVI KUMAR N V, BLANDIN J J, SUERY M, GROSJEAN E. Effect of alloying elements on the ignition resistance of magnesium alloys [J]. Scripta Materialia, 2003, 49(3): 225−230.

[9] LIU Sheng-fa, LI Bo, WANG Xiao-hu, SU Wei, HAN Hui. Refinement effect of cerium, calcium and strontium in AZ91

magnesium alloy [J]. Journal of Materials Processing Technology, 2009, 209(8): 3999−4004.
[10] LIU Xuan, XUE Ji-lai, ZHANG Peng-ju, WANG Zeng-jie. Effects of the combinative Ca, Sm and La additions on the electrochemical behaviors and discharge performance of the as-extruded AZ91 anodes for Mg-air batteries [J]. Journal of Power Sources, 2019, 414: 174−182.
[11] FLEMINGS M C. Behavior of metal many in the semisolid state [J]. Metallurgical Transactions B, 1991, 22: 269−293.
[12] STARKE E A, STALEY J T. Application of modern aluminum alloys to aircraft [J]. Progress in Aerospace Sciences, 1996, 32: 131−172.
[13] YANG Zhao, DONG Jian-xiong, ZHOU Li, SHEN Li, ZHANG Wei. A study of the method of manufacturing bimaterial composite parts through semisolid metal processing [J]. Metallurgical and Materials Transactions A, 2011, 42(6): 1709−1716.
[14] LU Shu-lin, WU Shu-sen, WAN Li, AN Ping. Microstructure and tensile properties of wrought Al alloy 5052 produced by rheo-squeeze casting [J]. Metallurgical and Materials Transactions A, 2013, 44(6): 2735−2745.
[15] ZHANG Yang, WU Guo-hua, LIU Wen-cai, ZHANG Liang, PANG Song, DING Wen-jiang. Preparation and rheo-squeeze casting of semi-solid AZ91−2wt.%Ca magnesium alloy by gas bubbling process [J]. Journal of Materials Research, 2015, 30(6): 825−832.
[16] FAN Jian-feng, YANG Chang-lin, HAN Gang, FANG Shuang, YANG Wei-dong, XU Bing-she. Oxidation behavior of ignition-proof magnesium alloys with rare earth addition [J]. Journal of Alloys and Compounds, 2010, 509(5): 2137−2142.
[17] FAN J F, YANG G C, CHEN S L, XIE H, WANG W, ZHOU Y H. Effect of rare earths (Y, Ce) additions on the ignition points of magnesium alloys [J]. Journal of Materials Science, 2004, 39(20): 6375−6377.
[18] HUTT J E C, STJOHN D H, HOGAN L, DAHLE A K. Equiaxed solidification of Al−Si alloys [J]. Materials Science and Technology, 1999, 15(5): 495−500.
[19] LU Li-ming, NOGITA K, MCDONALD S D, DAHLE A K. Eutectic solidification and its role in casting porosity formation [J]. JOM, 2004, 56(11): 52−58.
[20] HUNT J D. Steady state columnar and equiaxed growth of dendrites and eutectic [J]. Materials Science and Engineering A, 1984, 65(1): 75−83.
[21] LEE Young-chul, DAHLE A K, STJOHN D H. The role of solute in grain refinement of magnesium [J]. Metallurgical and Materials Transactions A, 2000, 31(11): 2895−2906.
[22] ONO N, NOWAK R, MIURA S. Effect of deformation temperature on Hall–Petch relationship registered for polycrystalline magnesium [J]. Materials Letters, 2004, 58(1): 39−43.
[23] CHOI Yung-ho, YOU Bong-sun, PARK Ik-min. Characterization of protective oxide layers formed on molten AZ91 alloy containing Ca and Be [J]. Metals and Materials International, 2006, 12(1): 63−67.
[24] CHEN Su-ling, YANG Gen-cang, FAN Jian-feng, LI You-jie, ZHOU Yao-he. Effect of Ca and Y additions on oxidation behavior of AZ91 alloy at elevated temperatures [J]. Transactions of Nonferrous Metals Society of China, 2009, 19: 299−304.
[25] LU Shu-lin, WU Shu-sen, DAI Wei, LIN Chong, AN Ping. The indirect ultrasonic vibration process for rheo-squeeze casting of A356 aluminum alloy [J]. Journal of Materials Processing Technology, 2012, 212(6): 1281−1287.
[26] CHUCHEEP T, BRUAPA R, JANUDOM S, WISUTMETHANGOON S, WANNASIN J. Semi-solid gravity sand casting using gas induced semi-solid process [J]. Transactions of Nonferrous Metals Society of China, 2010, 20: 1649−1655.

Ca 含量和流变挤压铸造工艺参数对 AZ91−1Ce−*x*Ca 合金显微组织和力学性能的影响

肖 然，刘文才，吴国华，张 亮，刘保良，丁文江

上海交通大学 材料科学与工程学院

轻合金精密成型国家工程中心和金属基复合材料国家重点实验室，上海 200240

摘 要：首先，研究不同 Ca 含量 AZ91−1Ce 合金的显微组织、力学性能和阻燃性能，优化出最佳 Ca 含量。然后，系统研究流变挤压铸造工艺参数(包括压力和转速)对 AZ91−1Ce−2Ca 合金显微组织和力学性能的影响。结果表明，随着 Ca 含量的增加，AZ91−1Ce−*x*Ca 合金的显微组织细化，阻燃性能提高。但当 Ca 含量超过 1%(质量分数)时，随着 Ca 含量的增加，AZ91−1Ce−*x*Ca 合金的力学性能迅速降低。在流变挤压铸造工艺中，压力和转速增加使 AZ91−1Ce−2Ca 合金的组织明显细化，气孔率降低，力学性能提高。与常规铸造相比，添加 2%Ca(质量分数)的 AZ91−1Ce 合金经流变挤压铸造成形后，不仅保证合金的抗氧化性(801 °C)，而且提高其力学性能。

关键词：Ca；AZ91−1Ce 合金；阻燃；流变挤压

(Edited by Bing YANG)